

Supplementary Information

Supplementary Methods

YGW diet feeding to mice with DEN induced HCC

Yang Gan Wan (YGW) and its starch control extracts were provided by SP Pharmaceutical. Animal experiments were performed in accordance with Institutional Animal Care and Use Committee-approved protocols. Two grams of YGW extract or the starch control were mixed with modified AIN-93G purified rodent diet with 2% (w/w) peanut flavor and pelleted according to the manufacturer's protocol (Dyets Inc., PA). Six-week old C57/B6j mice (Jackson Laboratory, ME) were fed with the YGW or control diet for 2 weeks and injected with 100 mg/kg of diethylnitrosamine (DEN) in saline (Sigma Aldrich, MO) intraperitoneally. The mice were given respective diet and 17.5% of Phenobarbital Elixir (0.07% of PB) (Qualitest, NC) in drinking water for 63 weeks. The weight and food intake were measured at the beginning of every month and the animals were sacrificed for assessment of the tumor incidence, mass, weight (n=10), and histology and CD133 expression (n=6). Tumors were graded blindly by a pathologist.

Immunoblotting

Cellular proteins were extracted with RIPA buffer containing protease and phosphatase inhibitors (Santa Cruz Biotechnology, CA). The extract was boiled in 6X SDS sample buffer. The lysate in sample buffer was separated by SDS electrophoresis and immunoblotted with indicated antibodies. For immunoblotting, primary antibodies

were purchased from the following sources: LC3 (2775), p62/SQSTM1 (5114), phospho- γ H2AX (Ser139) (2577), caspase-3 (9662), SAR1B (Pa5-28951) from Thermo Scientific, CA, RAB1B (sc-599), RAB14 (sc-98610), RAN (sc-1156), HA (sc-805) and β -actin (sc-47778) from Santa Cruz biotechnology, CA, RAB1A (11671-1-AP) from Proteintech, IL. All primary antibodies were incubated in 1:200 to 1:1000 dilutions in 5% BSA or 5% milk in TBST (Tris-HCL with 0.1% Tween20) buffer. The HRP conjugated secondary antibodies (Thermo Scientific, MA) were incubated in 5% milk TBST. The images were developed by X-ray films or Chemidoc Imager (Biorad, CA). The densitometry was performed in Chemidoc Imager.

MTT viability assay

The cells were treated in serum free TIC medium containing escalating concentration of compounds. At the end of assay, the cells were incubated with TIC culture medium with serum containing 0.5 mg/ml of MTT for four hours. The cells were lysed with MTT lysis buffer (15% SDS, 0.015 M HCl) and uptake of MTT was measured at 570 nm absorbance using a multi-well-reading UV-Vis spectrometer.

Lentivirus preparation

Lentiviruses were prepared by cotransfecting psPAX2 (Addgene), pMD2.G (Addgene) and a lentiviral vector together in 293FT cells (Life technologies, CA). To deplete SAR1B, pLKO.1-TRC (Sigma Aldrich, MO) carrying shRNAs targeting SAR1B, SAR1Bsh1 (TRCN0000100792), SAR1Bsh2 (TRCN0000100793), RAB1Bsh1 (TRCN0000302711) or RAB1Bsh2 (TRCN0000100824) were used to make lentiviruses. Supernatants of both virus preparations were used to infect 5×10^4 TICs in 6-well plates.

pLKO.1-puro non-target shRNA control plasmid was used as control. SAR1B lentiviral vector with C-terminal HA (LV503116) and control (LV587) from Applied Biological Materials was used to create HA-SAR1B expressing TICs. V5 tagged RAB1B in pLX304 lentiviral vector or control were obtained from DNASU plasmid repository. All cells were cultured in the presence of puromycin (Life technologies, CA) to create stable cell lines.

Anti-tumor analysis in nude mice

TICs (1×10^5) were inoculated subcutaneously in six week old nude mice (NCR Nu-M) purchased from Taconic, NY. One week after transplantation, the mice were treated with 20 mg/kg of CCI779 (1) and 20 mg/kg of BC or the combination or the vehicle intraperitoneally. The drugs were first dissolved in DMSO and further diluted in PBS before injection. Tumor volumes were measured with a caliper every other day and calculated as $(L \times M \times M)/2$.

Tunel staining

Tunel staining was performed by the Liver Histology Core of the USC Research Center for Liver Diseases, NIH grant No. P30-DK048522. Briefly, tissue sections were stained with tunel assay kit from Roche diagnostics according to the manufacturer's protocols.

Immunofluorescence microscopy

The cells were treated with compounds and subsequently fixed with 4% paraformaldehyde for 15 minutes at room temperature. After washing with PBS for 5

min three times in room temperature, the cells were blocked in blocking buffer (1XPBS/5%normal goat serum/0.3%Triton X-100) for 1 hr at room temperature. The cells were then incubated with primary antibody in antibody dilution buffer (1xPBS/1%BSA/0.3%Triton X-100) in 1:400 dilution at 4°C overnight and incubated with Alexa fluor 488 conjugated-secondary antibody (Cell Signaling, MA) for one hour at room temperature. The coverslips were mounted with mounting medium containing DAPI (Vectashield, CA) and the cells were imaged with Nikon Eclipse 90i microscope.

LC-MS Quantification of Components of YGW

C56/B6j mice were given 300 mg/kg of YGW extract in water by gavage. 300 mg YGW powder was suspended and vortexed briefly in 1 ml sterile water. After centrifugation, the soluble fraction was collected and diluted four times with sterile water. 100 µl of this extract was given to each 25 g mouse by gavage. At 0.25, 0.5, 1, 3, 6, 12, 24 hours after gavage, the mice were sacrificed for tissue collection. The plasma and liver were collected and immediately frozen in liquid nitrogen and kept at -80 °C. For the steady state study, the mice were given gavage of YGW extract once a day for seven consecutive days. The plasma and liver were collected at 1, 3, 6, 12, 24 hours after the last gavage.

The pharmacokinetics of YGW, BC, and Blin were all evaluated after an oral dosage of YGW, and at designated times, mice were euthanized, where blood and liver samples were collected. The plasma (50 µL) and liver samples were extracted using methanol protein precipitation. The livers were weighed, where approximately 45 mg of tissue was added to 100 µL of methanol and homogenized using a bullet blender. To

this mixture 100 μ L internal standard (Naringin, 10 μ g/mL) and 400 μ L methanol was added and further homogenized for 5 min. The samples are then centrifuged at 13000 rpm for 5 min, where 200 μ L of supernatant was transferred and 40 μ L injected into a Shimadzu Prominence linked onto Sciex API4000 operating the negative mode. The analytes were separated using Hypersil Gold C18 column (Thermo Scientific) with dimensions of 50 x 2.1 mm, 5 μ m particle size. BC, Blin and naringin were detected using signature multiple-reaction-monitoring (MRM) for each of the respective analyte.

Intracellular uptake and metabolism assay

TICs (5×10^6) were plated in 10, 10-cm dishes the day before treatment. Freshly isolated primary hepatocytes (2.4×10^6) for C57/B6j mice were plated in collagen-coated 10 cm dish for 2 hr at 37°C. The cells were treated with DMSO (0.1%), BC (30 μ M) and Blin (30 μ M) for two hours. The cells were washed with ice-cold PBS for two times and scraped off the plate in 5 ml of ice-cold PBS. They were centrifuged at 2500 rpm for 5 min at 4°C and lysed with 0.8 ml of ice-cold methanol. For the plates without cells, 0.8 ml of methanol was added to each plate and any bound compounds were scraped off the plates. The samples were centrifuged and the supernatants were collected and stored at -80°C. Proteins were extracted with RIPA buffer. Concentrations of BC and Blin in the cells were determined using the LC-MS assay as described in the above section.

Extract preparation, fractionation and compound identification

In order to extract bioactive metabolites from YGW, twenty grams of YGW powder was suspended in 200 ml of methanol for 2 days. Methanol soluble metabolites were

obtained after filtration of the insoluble material followed by evaporation of the methanol. The residue obtained (2.8 g) was then suspended in 100 ml of ddH₂O and partitioned with 100 ml of butanol twice to obtain water-soluble and butanol-soluble fractions. After evaporation of solvent, butanol fraction (750 mg) was found to be bioactive against TIC bioassay. The butanol fraction was subsequently chromatographed over 48.7 g of RP-18 gel (COSMOSIL 75C18-OPN, 30 × 80 mm, Nacalai, CA) eluting with MeOH-H₂O mixtures of decreasing polarity. Fraction A (200 ml of 10 % MeOH-H₂O, 174.1 mg), B (200 ml of 30 % MeOH-H₂O, 75.9 mg), C (200 ml of 70 % MeOH-H₂O, 347.8 mg), and D (200 ml of 100 % MeOH, 291.3 mg) eluted from RP-18 column were then subjected to TIC bioassay after evaporation of the solvent and fraction C was identified bioactive against TIC. Fraction C was further separated by a reverse phase semi-preparative HPLC column [Phenomenex Luna 5 μ m C18 (2), 250 × 10 mm] with a flow rate of 5.0 ml/min and measured by a UV detector at 254 nm. The gradient system was MeCN (solvent B) in 5 % MeCN/H₂O (solvent A): 30 to 50 % B from 0 to 20 min, 50 to 100 % B from 20 to 25 min, 100 % B from 25 to 30 min, 100 to 30 % B from 30 to 31 min, and re-equilibration with 30 % B from 31 to 35 min. Eluent was collected in a series of fractions with a 2 min interval with total of 14 fractions (from 2 to 30 min). Eluent collected from 14 to 16 min (fraction C7) showed a strongest and eluent from 20 to 22 min (fraction C10) showed a moderate bioactivity against TIC. Both fractions were then subjected to further purification and for LCMS, and 1D and 2D NMR analysis. The major compounds, baicalein (BC, 3.5 mg) and wogonin (Wog, 2.0 mg), were identified from fraction C7 and C10, respectively.

LCMS spectral data were collected on a ThermoFinnigan LCQ Advantage ion trap mass spectrometer, where analytes were separated using a RP C18 column (Alltech Prevail C18 2.1 × 100 mm with 3 μm particle size) at a flow rate of 125 μl/min with a 10 μl injection. The solvent gradient system and the conditions for MS analysis were as described (2). NMR data were collected on a Varian Mercury Plus 400 spectrometer. The structures of baicalein and wogonin were elucidated by their mass, ¹H-, ¹³C-, and 2D-NMR data and confirmed by comparing their spectroscopic data with those of literatures (3, 4) as well as commercial authentic samples purchased from Sigma Aldrich.

Computer modeling of BC and GTPase interaction

Three-dimensional structures of SAR1B (PDB code: 1F6B) and Rab1b:TBC1D20_1-305 (PDB code: 4HLQ) were used as a template to search for putative binding sites of BC. In preparation for ligand binding studies, an initial model was generated using SWISS-MODEL¹⁻⁴ web server to build the missing residues in the crystal structure of SAR1B. Prime module in Schrodinger (Schrodinger, Inc., MA) was additionally used to find an optimal conformation of the missing residues in the crystal structure. The final structural model was obtained after a cycle of minimization followed by a short molecular simulation. Putative binding site of small molecules was identified with site score 0.721 (DScore=0.693) using Sitemap module. Subsequent binding studies were performed using Glide. Figures were produced using ChemDraw (CambridgeSoft, MA).

Immunohistochemistry

Tissue slides were deparaffinized with xylene/ethanol washed. The slides were boiled in citrate antigen retrieval solution. After blocking, the slides were incubated with LC3 antibody (3868, Cell Signaling) over night. Immunohistochemistry was performed the next day.

RNA extraction and Quantitative PCR analysis

RNA from cells was isolated using Quick-RNA MiniPrep kit (Zymo research, CA) and RNA from liver and tumor tissues using Direct-zol RNA MiniPrep kit (Zymo research, CA). The first-strand cDNA synthesis was performed by maxima first strand cDNA synthesis kit (Thermo scientific, CA) using 1 µg of total RNA. The qPCR analysis was performed with a proper set of primers for each gene of interest and fast SYBR green mastermix (Life technologies, CA) with the standard cycle in Viia7 instrument (Life technologies, CA). The relative RNA expression was analyzed by the delta delta Ct method.

Primers used for qPCR

Symbol	Primer Sequences
<i>m-Alb</i>	F-5'-TGAGTGAGCATGTTACCAA-3'(5)
	R-5'-AGAGCAGAGAAGCATGGC-3'
<i>m-Cyp7a1</i>	F-5'-ATGTATGCCTTCTGCTACCG-3'(5)
	R-5'-ATCTTTGCCAAACAGCGTTAGA-3'
<i>m-36B4</i>	F-5'-AGATTCGGGATATGCTTGTTGGC-3'(5)
	R-5'-TCGGGTCCTAGACCAGTGTTTC-3'

<i>m-Nanog</i>	F-5'-AGGGTCTGCTACTGAGATGCTCTG-3'(5)
	R-5'-CAACCACTGGTTTTTCTGCCACCG-3'
<i>m-Sox2</i>	F-5'-GGCAGCTACAGCATGATGCAGGAGC-3'(5)
	R-5'-CTGGTCATGGAGTTGTACTGCAGG-3'
<i>m-Tlr4</i>	F-5'-GGCAACTTGGACCTGAGGAG-3'(5)
	R-5'-CATGGGCTCTCGGTCCATAG-3'
<i>m-CD133</i>	F-5'-CTGGGAGGCAGAATAAAGGA-3'(5)
	R-5'-GGTTGGTATTGAGCTGGGTG-3'
<i>m-Twist1</i>	F-5'-GGACAAGCTGAGCAAGATTCA-3'(6)
	R-5'-CGGAGAAGGCGTAGCTGAG-3'
<i>m-Snai1</i>	F-5'-CACACGCTGCCTTGTGTCT-3'(6)
	R-5'-GGTCAGCAAAGCACGGTT-3'

Real-time PCR

Real time PCR of human CD133 was performed according to protocol described before (7). cDNA was synthesized from 1 µg of total RNA as described above. Real time PCR was performed by 2X GoTaq green master mix (Promega, WI) with the proper set of primers in a thermal cycle programmed with one cycle at 95°C for 5 min, 28 cycles at 94°C for 1 min, 50°C for 1 min, and 72°C for 1 min, and ending with one cycle at 72°C for 5 min. Amplified products were resolved and visualized on a 2% agarose gel.

Primers used for real-time PCR

Symbol	Primer Sequences
<i>h-CD133</i>	F-5'-ACATGAAAAGACCTGGGGG-3'
	R-5'-GATCTGGTGTCCCAGCATG-3'
<i>h-β-actin</i>	F-5'-ATCTGGCACCACACCTTCTA-3'
	R-5'-CTCGGTGAGGATCTTCATGA-3'

Figure Legends

Fig S1: Yang Gan Wan (YGW) prevents chemically induced liver tumor. A) Experimental outline for testing YGW or control diet in a mouse model of HCC. Male C57/B6j mice were fed YGW containing diet (n=10) or control diet (n=10). Liver tumors were induced with the DEN/phenobarbital regimen for 67 wk before sacrificing for analysis. B) The mice fed with YGW and control diets grew comparably. C) Tumor incidence (n=10). D) Total liver/body weight fraction (n=10). E) Representative photos of livers. F) Total tumor mass (n=10). G) Representative microphotographs of liver sections stained with H&E. Scale bars represent 100 μm. H) Histological tumor score blindly assigned by a pathologist (n=6). I) CD133 mRNA expression of non-tumor liver tissues (n=6). Statistical comparisons were performed by two-tailed t-test. Brackets indicate SEM of replicate experiments. J) Selective toxicity of YGW on TICs vs. freshly isolated mouse hepatocytes (mHep). The cells were treated with escalating concentration of YGW extract for 4 days and MTT assay was performed to measure viability (n=6 for each concentration). K) Selective induction of apoptotic markers in TICs vs. freshly isolated mouse hepatocytes as assessed by immunoblotting of analysis. The

cells were treated with escalating concentration of YGW extract for 24 hr and immunoblotted with indicated antibodies. L) Effects of YGW extract on spheroid formation of TICs. TICs were treated YGW extract or vehicle in spheroid culture conditions for 7 days and colonies were counted. Scale bars represent 400 μm . M) Gene expression analysis of TICs treated with YGW extract vs. control extract for 24 hr by qPCR analysis (n=3). All statistical comparison was performed by One-way ANOVA with Bonferroni post-test. Error bars represent SEM. * $p < 0.05$ and ** $p < 0.01$.

Fig S2: A) The diet consumption and the weight of mice were measured during the first week of every month. B) The YGW consumption amount was calculated from the the amount of diet consumed and the the concentration of YGW in the diet. Average values of 5 mice per group and two groups for each diet are shown.

Fig S3: The liver pictures of DEN-fed with A) control, B) YGW diets. Visible tumors are shown in red arrows.

Fig S4: Spectrometric characterizations of buthanol fraction C7 of YGW. A) UV-Vis and B) mass spectra of buthanol fraction C7. ^1H NMR spectra of C) fraction C7 and D) BC from Sigma Aldrich.

Fig S5: Pharmacokinetics of Baicalein (BC) and Baicalin (Blin). Liver concentrations of BC and Blin at various times after a single oral gavage (A) or daily gavage for 7 consecutive days (B) of YGW (300 mg/kg). C) and D) Plasma concentrations of BC and Blin in the same groups of mice shown above. E) Intracellular concentrations of BC and Blin after treating TICs and freshly isolated mHep with BC for 2 hr. F) Percent conversion of BC to Blin after BC treatment in TICs and mHep. G) Intracellular

concentrations of BC and Blin after treating TICs and primary mHep with Blin. H) Percent conversion of Blin to BC after Blin treatment in TICs and mHep. Error bars represent SEM of triplicate experiments. * $p < 0.05$ and ** $p < 0.01$.

Fig S6: Baicalein enhances cytotoxicities of TICs induced by A) sorafenib (sora), B) doxorubicin (dox), C) rapamycin (rapa) and D) temsirolimus (CCI779). TICs were treated with indicated compounds for 4 days and MTT assay was performed to measure the viability. Means and SEMs of six replicates are shown, and one- or two-way ANOVA analysis was performed with Bonferroni post-test to determine the statistical significance. * $p < 0.05$ and ** $p < 0.01$.

Fig S7: TICs are treated with CCI779 (10 μ M), Baicalein (30 μ M) or the combination for 24 hr. QPCR analysis was performed for A) *Nanog* and B) *Sox 2*.

Fig S8: CCI779 enhanced BC induced apoptosis specifically in HCC cells. Huh7 and hHep cells were treated with or without 5 μ M CCI779 and different concentrations of CCI779 for 24 hr. The cell lysates were immunoblotted with caspase 3 antibody.

Fig S9: Structural depiction of nano-bead conjugation. The sites of conjugation are highlighted in the red boxes.

Fig S10: Mechanism of inhibition of GTP binding pocket by BC. A) GTP competitively blocks Blin (B)-nanobead pulldown of RAB1A. B) BC blocks GTP pulldown of RAB1B from RAB1B overexpressing cell lysates. C) Three dimensional modeling of baicalein's binding to SAR1B. The ribbon representation of hamster SAR1B is modeled with GTP in rainbow color and BC in brown color. The N-terminus is blue and C-terminus is brown. D) The surface model of SAR1B is shown in pink with GTP shown in green stick

model and BC shown in brown stick model in a binding pocket in a region known as the Sar1-NH₂-terminal activation recruitment (STAR)(8). E) Putative interacting residues of SAR1B with BC are shown with arrows indicating hydrogen bonds. F) Three dimensional simulation of interaction between BC and RAB1:TBC1D20 complex (9). G) Predicted molecular mechanisms of interaction between BC and the conserved residues in RAB1B.

Fig S11: Amino acid sequences of selected RAB proteins and SAR1B. The residues predicted to interact with BC in computer modeling are shown in colors. Specific conserved residues from RAB1A and RAB1B are shown in green. Conserved residues among RAB proteins and SAR1B are shown in red.

Fig S12: A) TICs were treated with YGW and BC for 24 hr and immunoblotted with anti-p62/SQSTM1 antibody. YGW and BC caused p62/SQSTM1 accumulation, a typical feature of autophagy inhibition. B) Hydroxyl groups on 5, 6, 7 positions of flavone were critical for autophagy inhibition. TICs were treated with indicated compounds for 2 hr and immunoblotted with indicated antibodies. The experiment was repeated for 5 times and LC3II densitometry was performed. One-way ANOVA analysis with Bonferroni post-test was performed to determine statistical significance between different experimental groups. * $p < 0.05$.

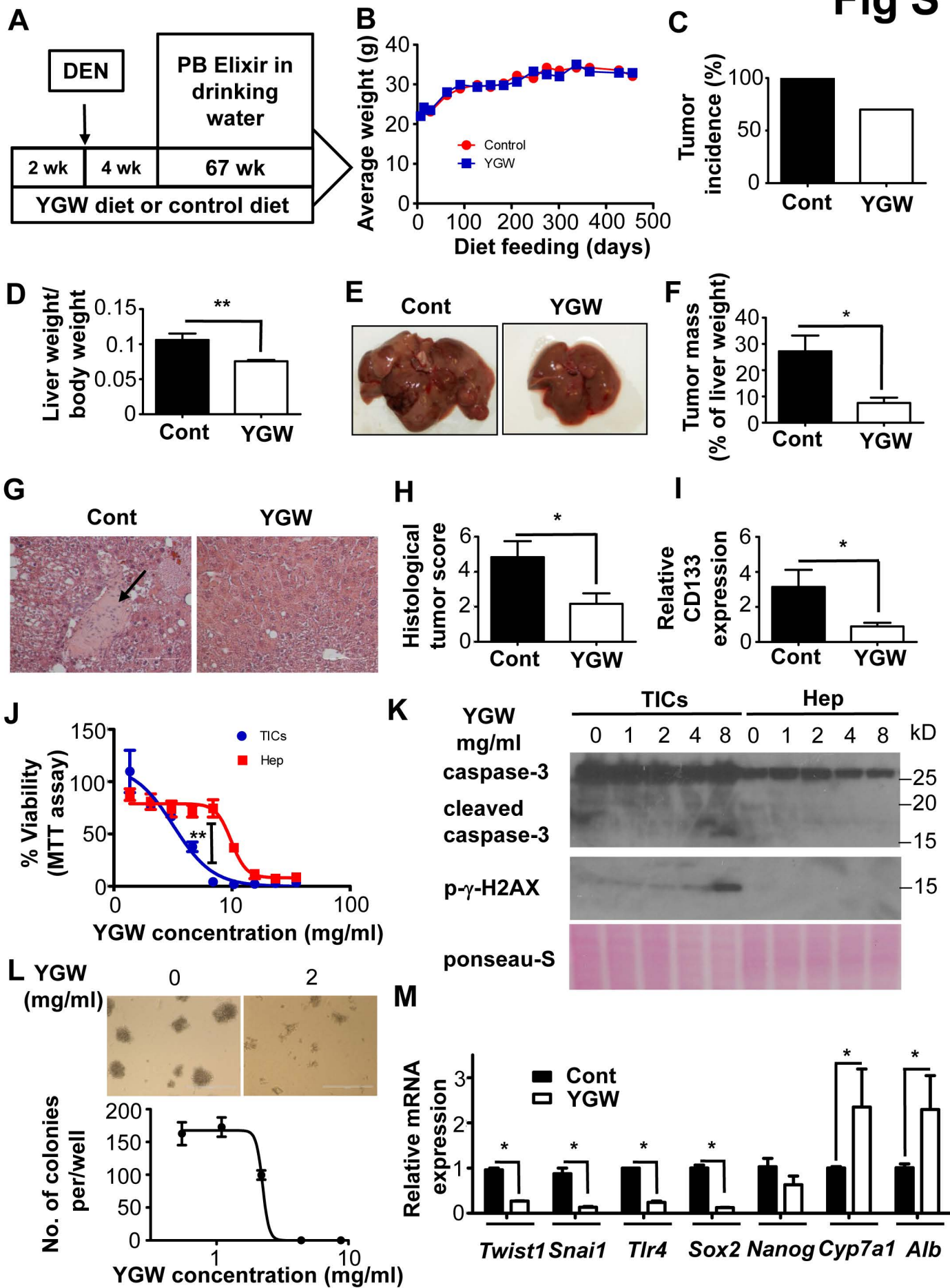
Fig S13: Baicalein enhances anti-TIC activity of mTORC1 inhibitor *in vivo*. TIC-derived tumor volumes were measured in nude mice after subcutaneous TIC transplantation. The arrows indicate the times when the compounds were given to the nude mice intraperitoneally. For quantitative data, means and SEMs are shown, and one- or two-

way ANOVA analysis was performed with Bonferroni post-test to determine the statistical significance. * $p < 0.05$ and ** $p < 0.01$.

Fig S14: A) TICs infected with shRNAs against RAB1B and SAR1B were treated with CCI779 (10 μM) for 2 hr and immunoblot analysis was performed with indicated antibodies. B) TICs were infected with V5-LACZ or V5-RAB1B. The cells were treated with CCI779 (10 μM) and BC (30 μM) for 2 hr and immunoblot analysis was performed with indicated antibodies. C) TICs were treated with CCI (10 μM), BC (30 μM) or a combination for 7 days and the surviving cells were replated and allowed to grow for another 7 days.

References

1. Bray K, Mathew R, Lau A, Kamphorst JJ, Fan J, Chen J, Chen HY, et al. Autophagy suppresses RIP kinase-dependent necrosis enabling survival to mTOR inhibition. *PLoS One* 2012;7:e41831.
2. Bok JW, Chiang YM, Szewczyk E, Reyes-Dominguez Y, Davidson AD, Sanchez JF, Lo HC, et al. Chromatin-level regulation of biosynthetic gene clusters. *Nat Chem Biol* 2009;5:462-464.
3. Qin L, Markham KR, Pare PW, Dixon RA, Mabry TJ. Flavonoids from elicitor-treated cell suspension cultures of *Cephalocereus senilis*. *Phytochemistry* 1993;32:925-928.
4. Morimoto M, Tanimoto K, Nakano S, Ozaki T, Nakano A, Komai K. Insect antifeedant activity of flavones and chromones against *Spodoptera litura*. *J Agric Food Chem* 2003;51:389-393.
5. Chen CL, Tsukamoto H, Liu JC, Kashiwabara C, Feldman D, Sher L, Dooley S, et al. Reciprocal regulation by TLR4 and TGF- β in tumor-initiating stem-like cells. *J Clin Invest* 2013;123:2832-2849.
6. Li Y, Wang J, Asahina K. Mesothelial cells give rise to hepatic stellate cells and myofibroblasts via mesothelial-mesenchymal transition in liver injury. *Proc Natl Acad Sci U S A* 2013;110:2324-2329.
7. Won C, Kim BH, Yi EH, Choi KJ, Kim EK, Jeong JM, Lee JH, et al. Signal transducer and activator of transcription 3-mediated CD133 up-regulation contributes to promotion of hepatocellular carcinoma. *Hepatology* 2015;62:1160-1173.
8. Huang M, Weissman JT, Beraud-Dufour S, Luan P, Wang C, Chen W, Aridor M, et al. Crystal structure of Sar1-GDP at 1.7 Å resolution and the role of the NH2 terminus in ER export. *J Cell Biol* 2001;155:937-948.
9. Gavriljuk K, Gazdag EM, Itzen A, Kötting C, Goody RS, Gerwert K. Catalytic mechanism of a mammalian Rab-RabGAP complex in atomic detail. *Proc Natl Acad Sci U S A* 2012;109:21348-21353.



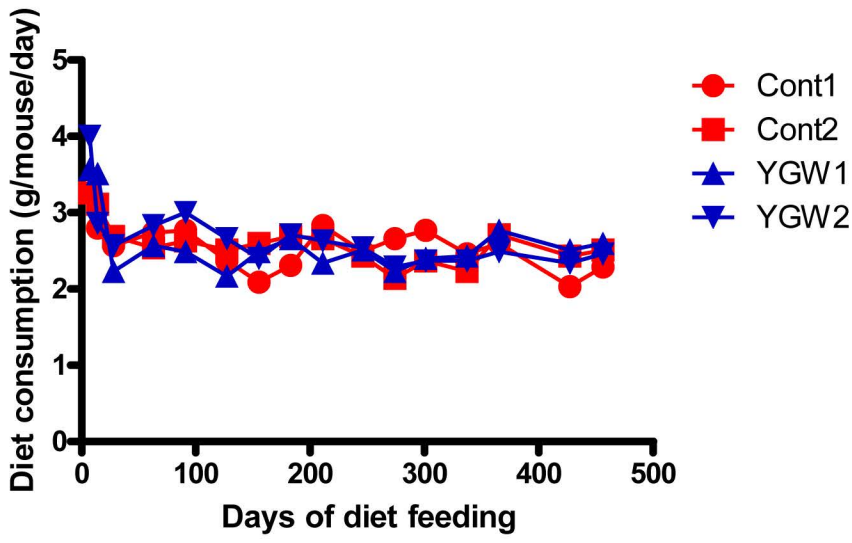
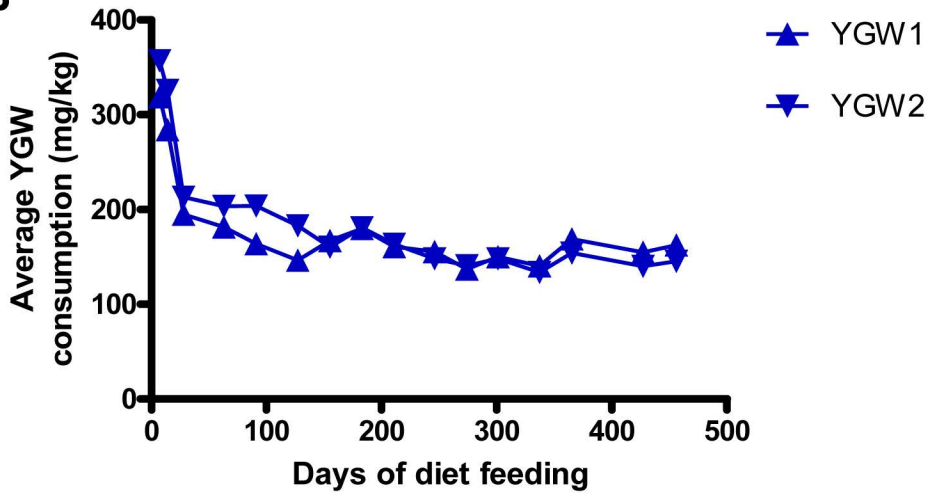
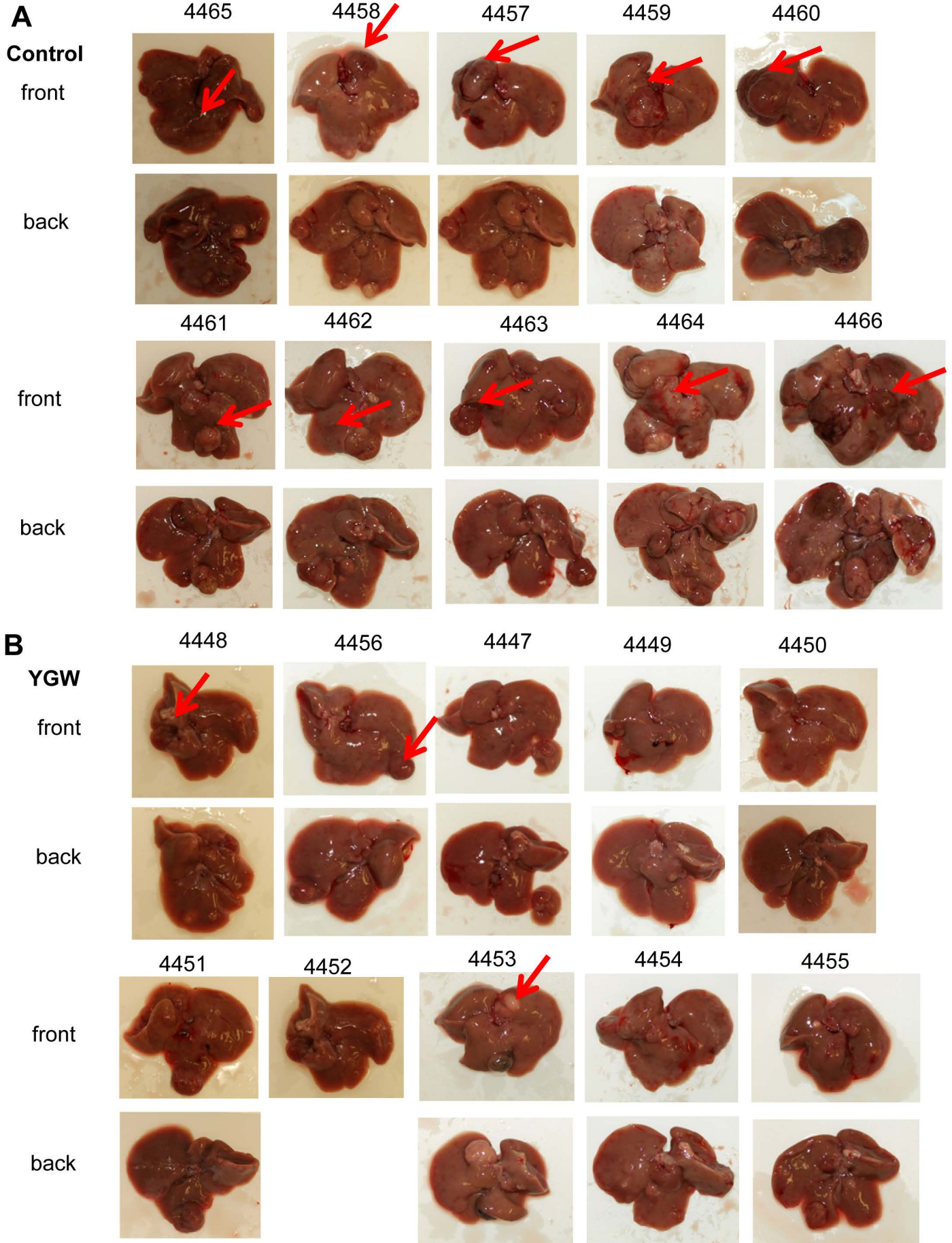
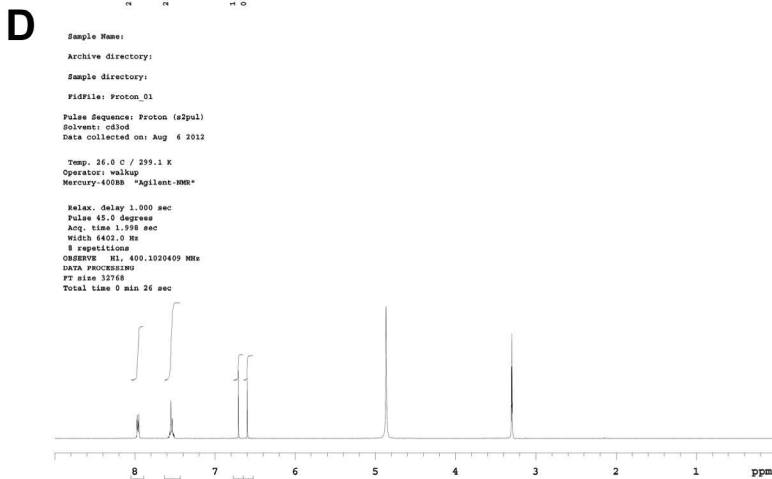
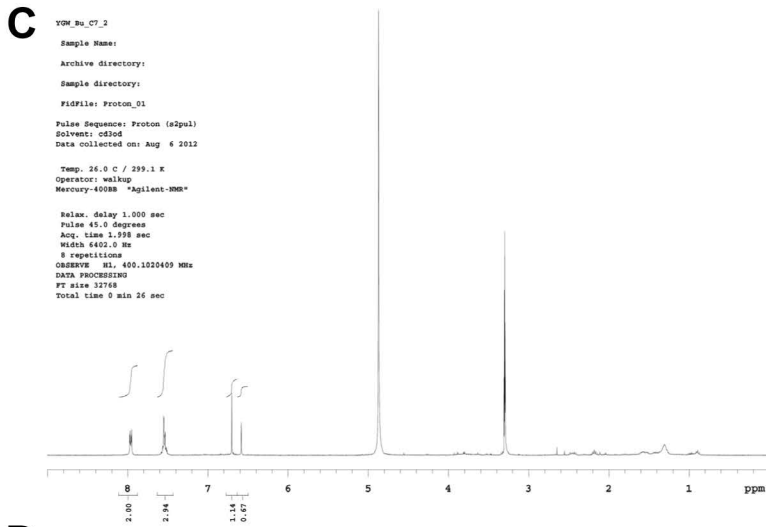
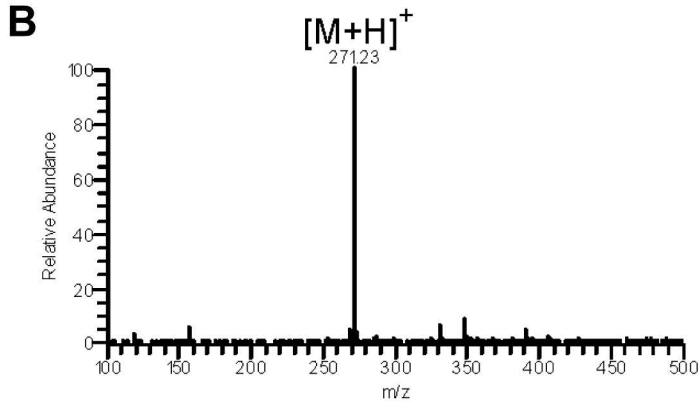
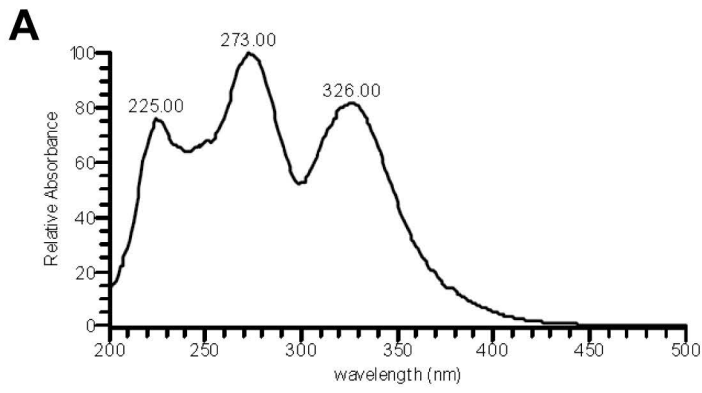
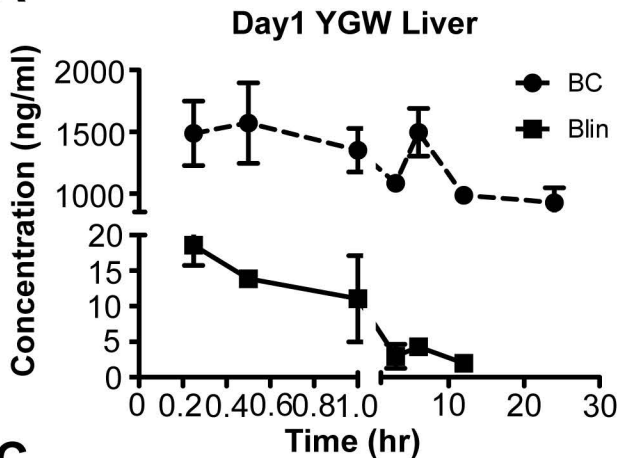
A**B**

Fig S3

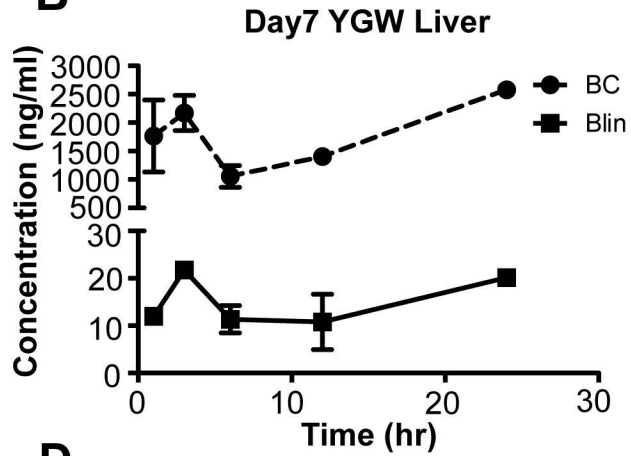




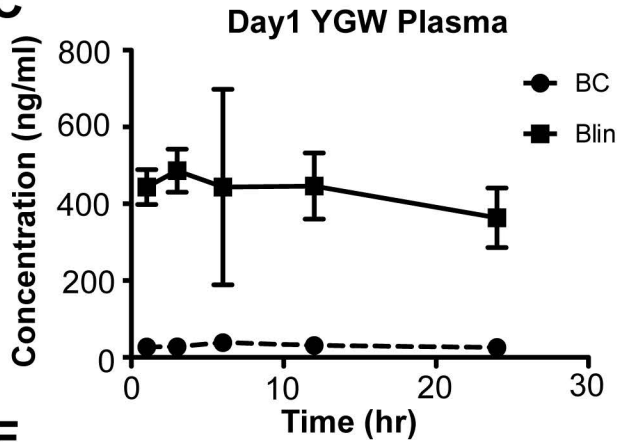
A



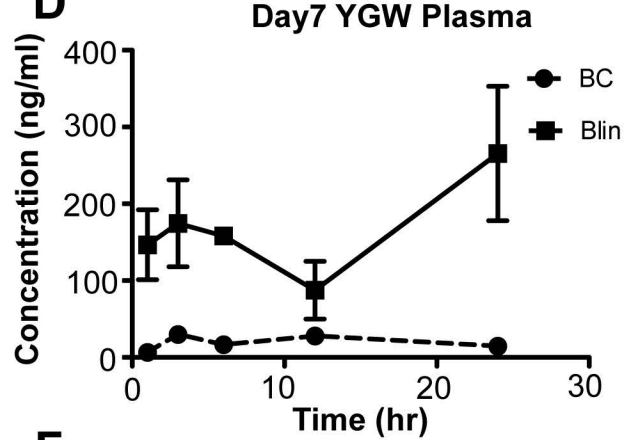
B



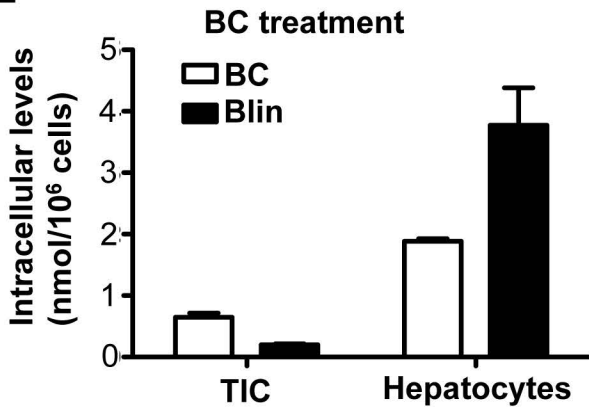
C



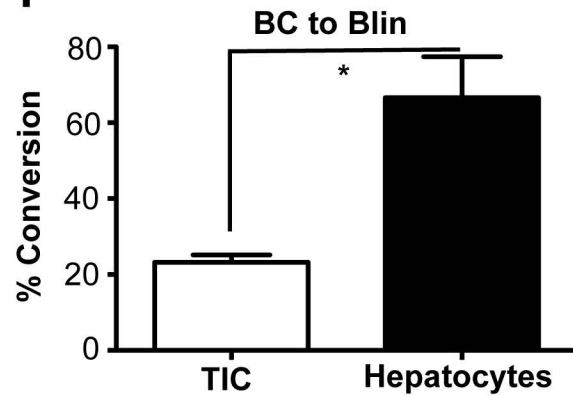
D



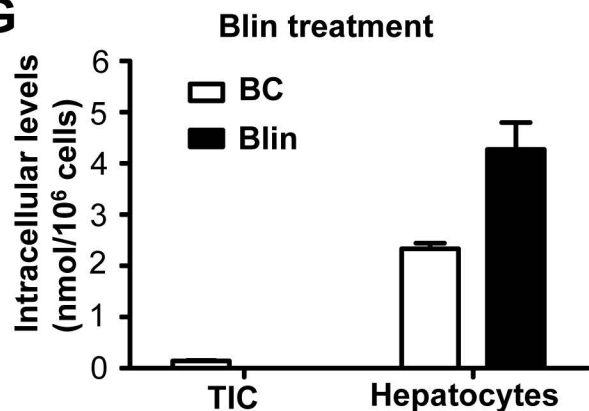
E



F



G



H

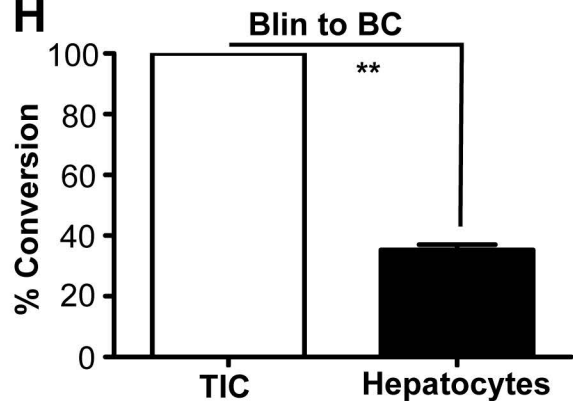
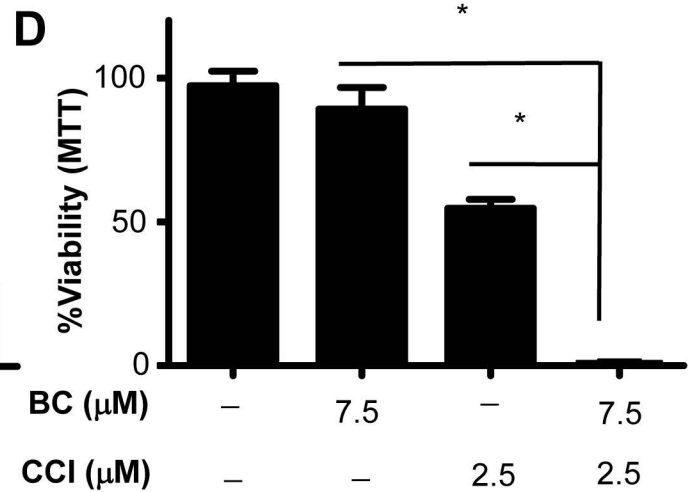
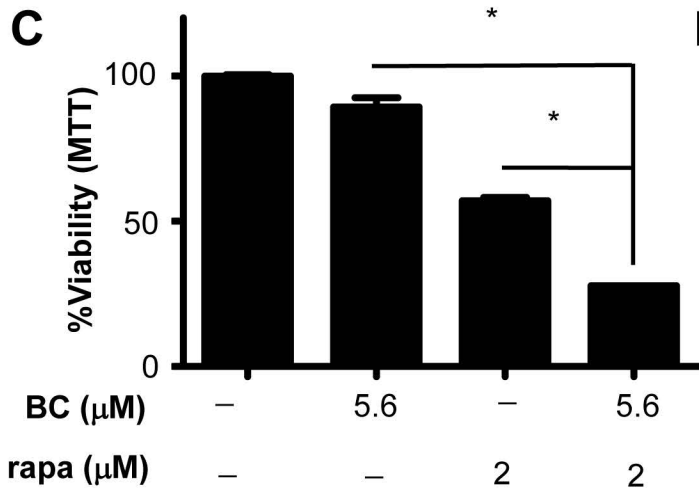
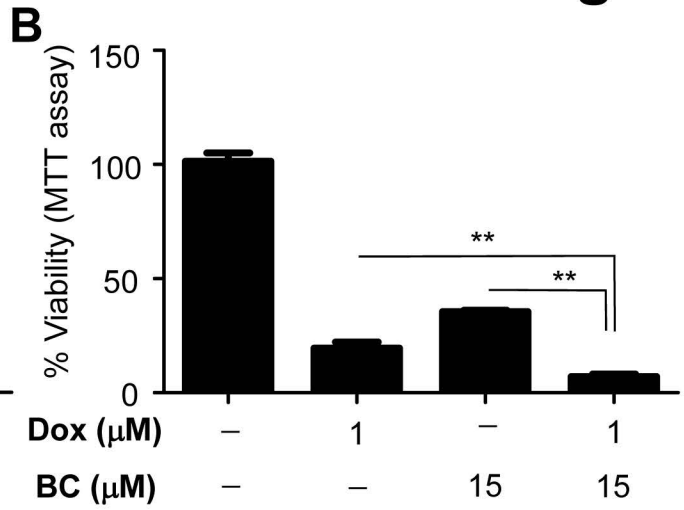
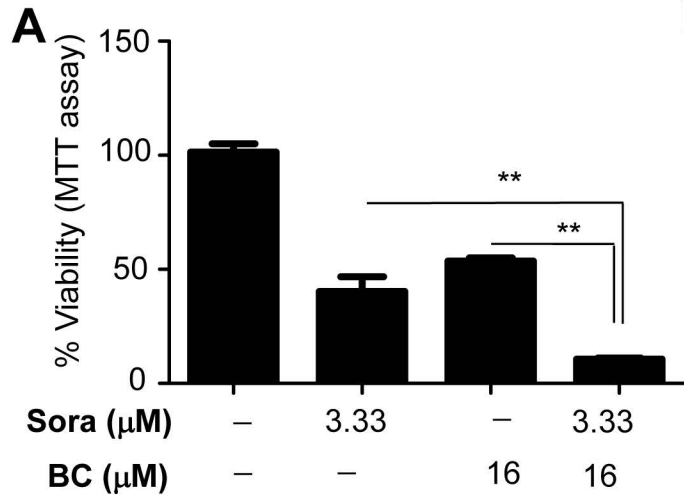


Fig S6

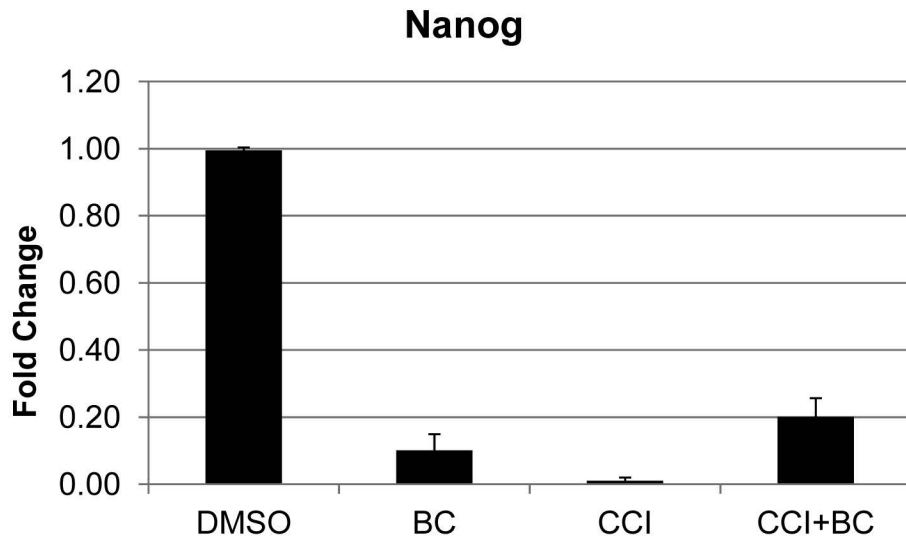
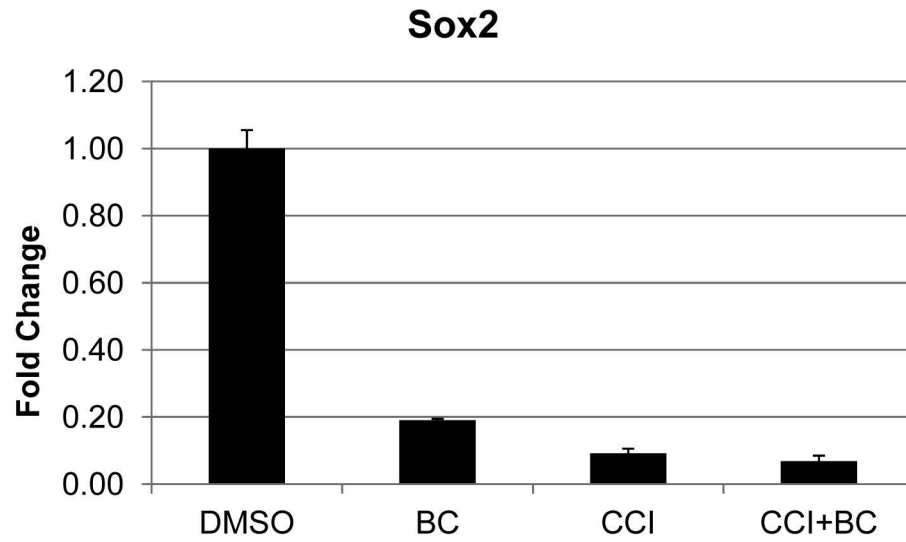
A**B**

Fig S8

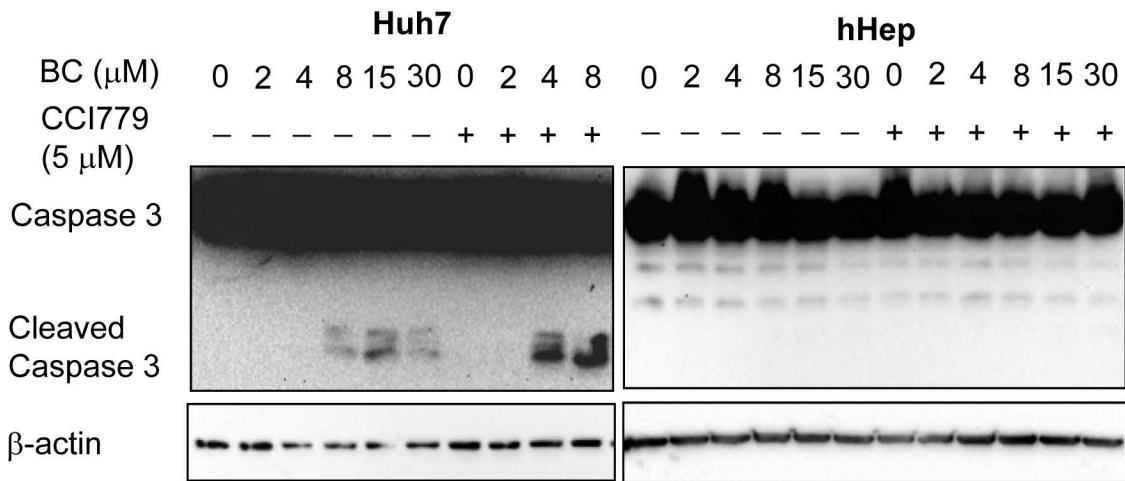
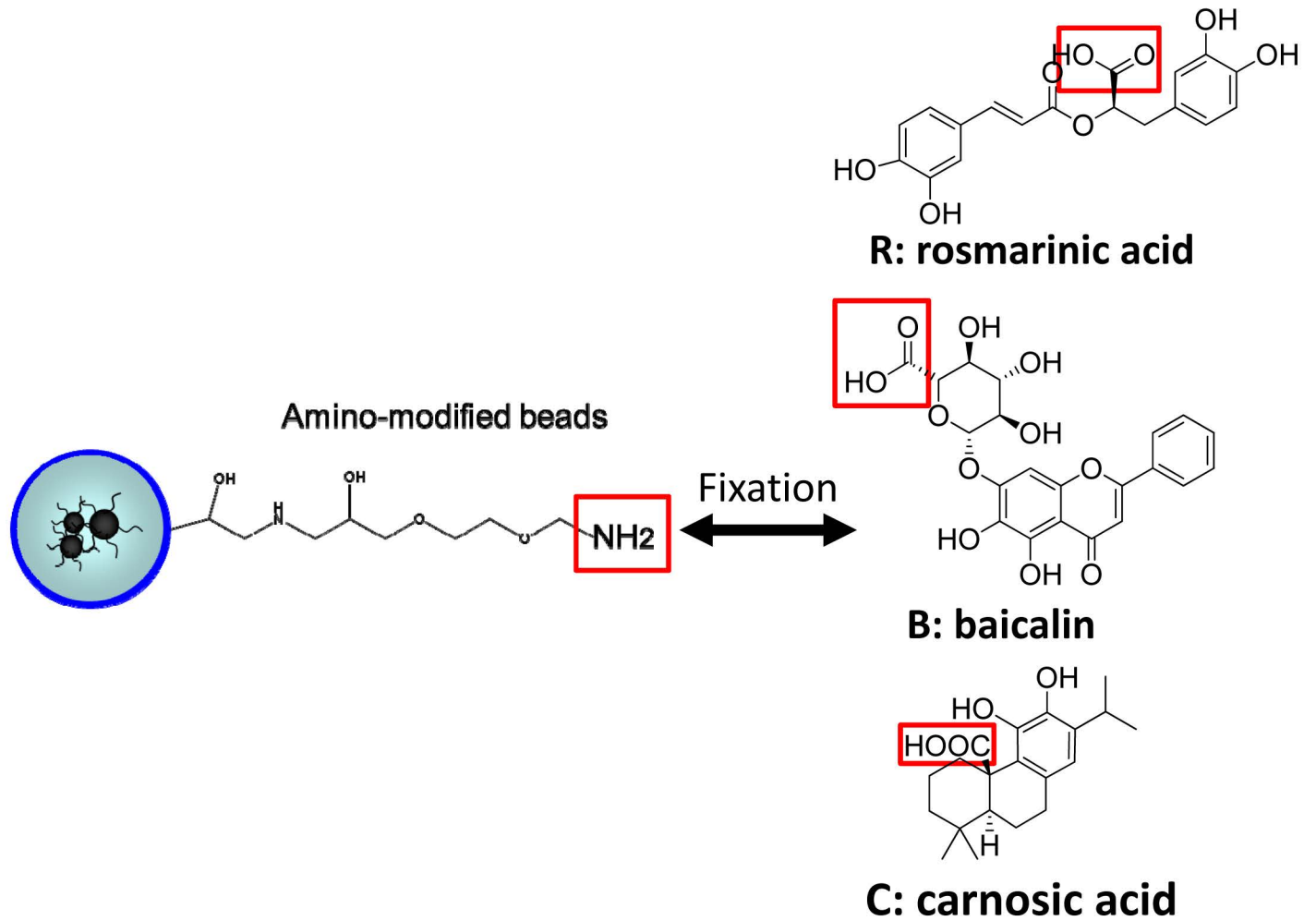


Fig S9



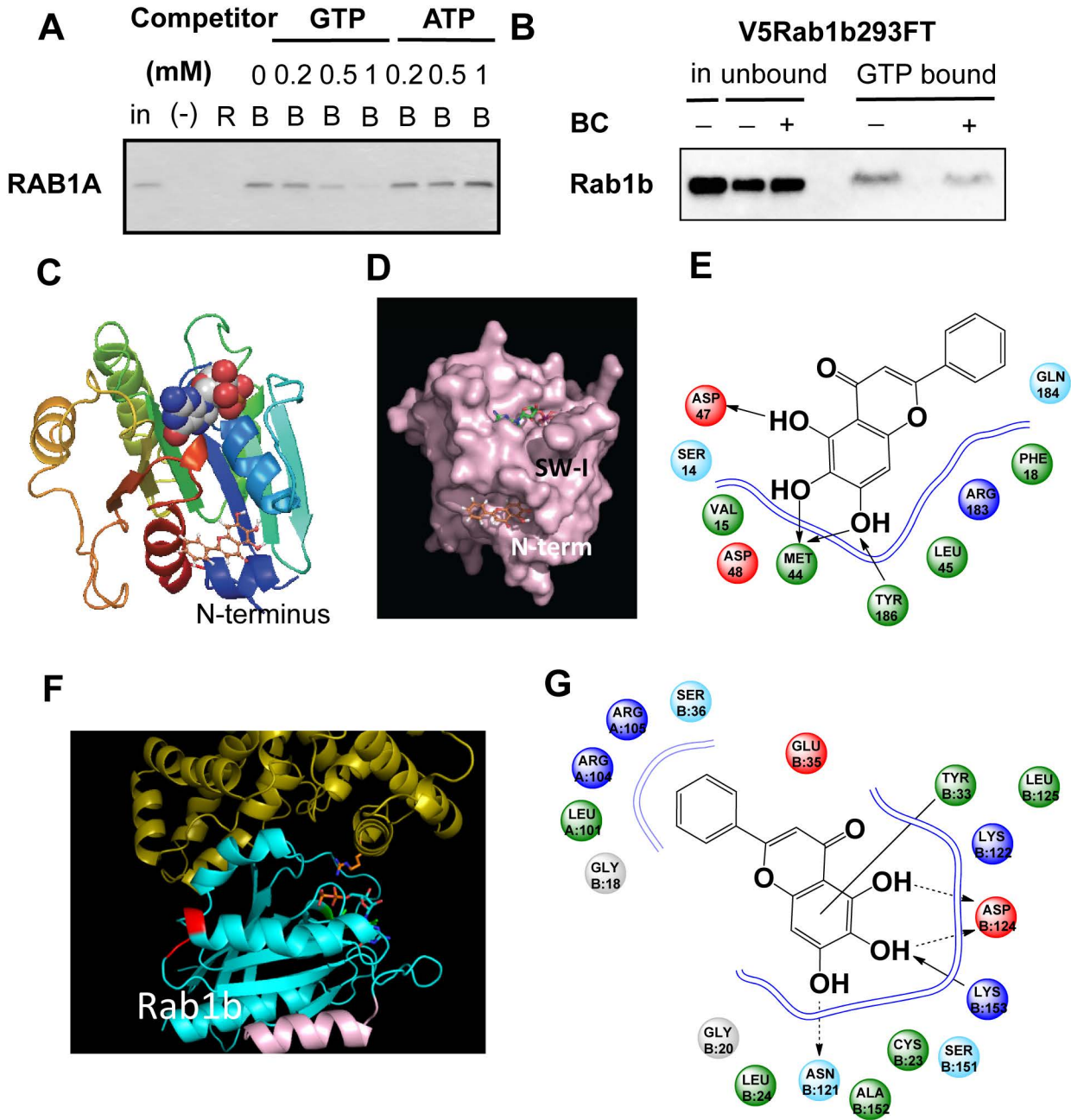


Fig S11

Mouse RAB1A MSSMN----PEYD-----YLFKLLLIGDSGVGKSCLLLRFADDTYTESYISTIGVDFKI
Mouse RAB1B MN----PEYD-----YLFKLLLIGDSGVGKSCLLLRFADDTYTESYISTIGVDFKI
Mouse RAB14 MATAPYNYS-----YIFKYIIIGDMGVGKSCLLHQFTEKKFMADCPHTIGVEFGT
Mouse RAB5A MANRGATRPNPNTGNKICQFKLVLLGESAVGKSSLVLRVFKGQFHEFQESTIGAAFLT
Mouse RAB5B MTSRSTARPNQPQASKICQFKLVLLGESAVGKSSLVLRVFKGQFHEYQESTIGAAFLT
Mouse RAB7 MTSRK-----KVLKLVIIIGDSGVGKTSLMNQYVNNKFSNQYKATIGADFLT
Mouse SAR1B MSFIFDWIYSGFSSVLQFLGLYKKSGLVFLGLDNAGKTTLLHMLKDDRLGQHVPTL

Mouse RAB1A RTIELDGKTIKLIQIWDTAGQERFRTITSSYYRGAHGIIVVYDVTQESFNNVKQWLQEID
Mouse RAB1B RTIELDGKTIKLIQIWDTAGQERFRTITSSYYRGAHGIIVVYDVTQESYANVKQWLQEID
Mouse RAB14 RIIEVSGQKIKLIQIWDTAGQERFRAVTRSYYRGAAGALMVYDITRRSTYNHLSSWLT DAR
Mouse RAB5A QTVCLDDTTVKFEIWDTAGQERYHSLAPMYRGAQAIVVYDITNEESFARAKNWKELQ
Mouse RAB5B QSVCLDDTTVKFEIWDTAGQERYHSLAPMYRGAQAIVVYDITNQETFARAKTWVKELQ
Mouse RAB7 KEVMVDDRLVTMQIWDTAGQERFQSLGVAFYRGADCCVLVFDVTAPNTFKTLDSWRDEFL
Mouse SAR1B HPTSEELTIAGMTFTTDFDLGGHVQARRVWKNYLPAINGIVFLVDCADHERLLESKEEL

Mouse RAB1A RYAS----ENVNKL LVGNKCDLTTKKVVDYTTAKEFADSLGIPFLETSAKNATNVEQSFM
Mouse RAB1B RYAS----ENVNKL LVGNKSDLTTKKVVDNTTAKEFADSLGVPFLETSAKNATNVEQAFM
Mouse RAB14 NLTNPNTV IILIGNKADLEAQRDVTYEEAKQFAEENGLLFLEASAKTGENVEDAFL
Mouse RAB5A RQAS----PNIVIALSGNKADLANKRAVDFQEAQSYADDNSLLFMETSAKTSMNVNEIFM
Mouse RAB5B RQAS----PSIVIALAGNKADLANKRMVEYEEAQAYADDNSLLFMETSAKTAMNVNDLFL
Mouse RAB7 IQASRPDPENFPFVVLGNKIDL ENRQVATKRAQAWCYSKNNIPYFETSAKEAINVEQAFQ
Mouse SAR1B DSLMTDETIANVPILILGNKIDRPEAISEERLREMFLYQGTTGKGSVSLKELNARPLEVF

Mouse RAB1A TMAAEIKKRMGPGATAGGAEKSNVKIQSTPVKQSGGGCC
Mouse RAB1B TMAAEIKKRMGPGAASGGERPNLKIDSTPVKPASGGCC
Mouse RAB14 EAAKKIYQNIQDGS LDLNAAESGVQHKPSAPQGGRLTSEPQPQREGCGC
Mouse RAB5A AIAKKLPKNEPQNPGANSARGRGVDLTEPAQPARSQCCSN
Mouse RAB5B AIAKKLPKSEPQNLGGAAGRSRGVDLHEQSQQNKSQCCSN
Mouse RAB7 TIARNALKQETEVELYNEFPPEPIKLDKNDRAKASAESCSC
Mouse SAR1B MCSVLKRQGYGEGFRWMAQYID

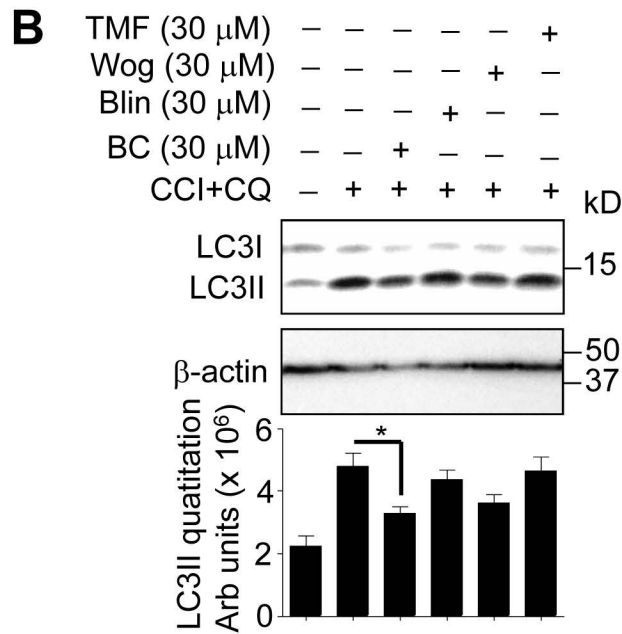
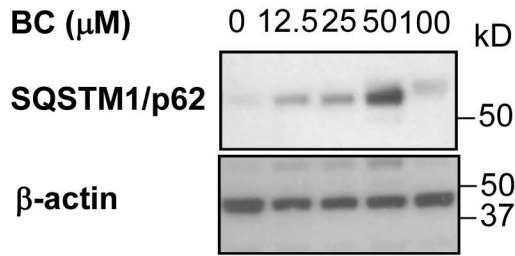
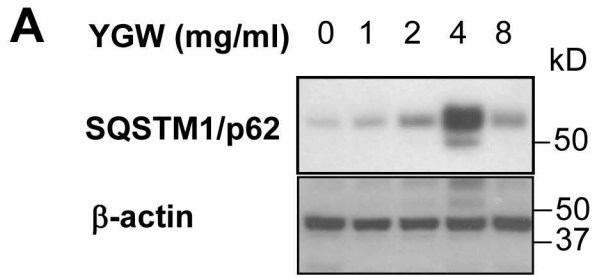
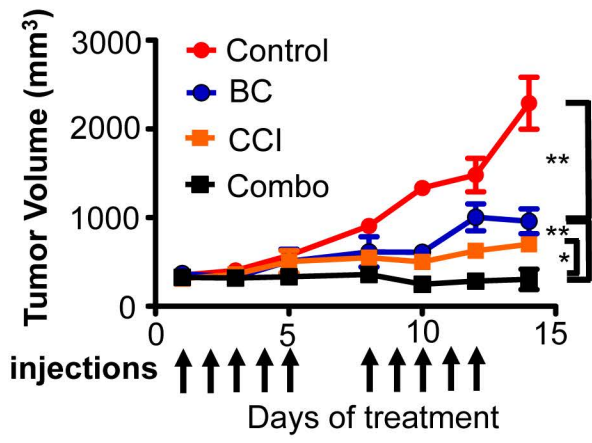
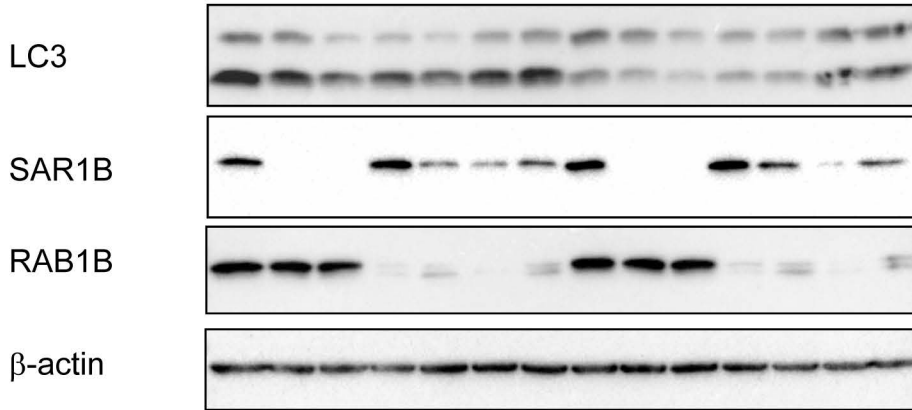


Fig S13



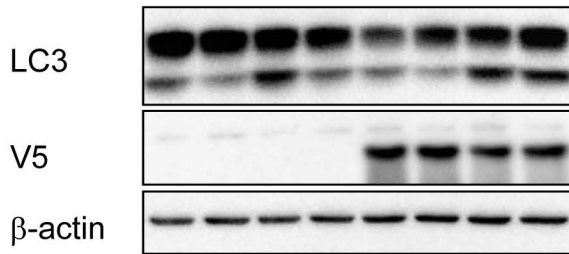
A

CCI779(10 μ M)	+	+	+	+	+	+	+	-	-	-	-	-	-	-
scrambledsh	+	-	-	-	-	-	-	+	-	-	-	-	-	-
RAB1Bsh2711	-	-	-	-	+	-	+	-	-	-	-	+	-	+
RAB1Bsh0824	-	-	-	+	-	+	-	-	-	-	+	-	+	-
SAR1Bsh0792	-	-	+	-	-	-	+	-	-	+	-	-	-	+
SAR1Bsh0793	-	+	-	-	-	+	-	-	+	-	-	-	+	-



B

	V5-LacZ				V5-RAB1B			
CI (10 μ M)	-	-	+	+	-	-	+	+
BC (30 μ M)	-	+	-	+	-	+	-	+



C

